ICROS-SICE International Joint Conference 2009
August 18-21, 2009, Fukuoka International Congress Center, Japan

A Study on the Discretization of a Distributed RC Circuit Model

Kentaro TAKAGI[1], Ichiro JIKUYA[1], Gou NISHIDA[2],
Bernhard MASCHKE[3], Kinji ASAKA[4]

[1]Department of Mechanical Science and Engineering, Nagoya University, Nagoya, Japan
(Tel: +81-52-789-2754/3289; E-mail: takagi@nuem.nagoya-u.ac.jp/jikuya@nuae.nagoya-u.ac.jp)
[2]RIKEN-TRI Collaboration Center, RIKEN, Nagoya, Japan
(Tel: +81-52-736-5870; E-mail: nishida@nagoya.riken.jp)
[3]Université Lyon 1, CNRS, UMR 5007, LAGEP, Villeurbanne, F-69622, France
(Tel: +33-4-7243-1842; E-mail: maschke@lagep.univ-lyon1.fr)
[4]Research Institute for Cell Engineering, AIST, Osaka, Japan
(Tel: +81-72-751-9180; E-mail: asaka-kinji@aist.go.jp)

Abstract: This paper discusses the mixed finite-element based Hamiltonian discretization of a distributed RC circuit aimed at modeling the impedance of rough electrodes of ionic polymer actuators. The accuracy of the discretized model is discussed by comparing the frequency responses between the discretized and the exact solution in the case of the constant impedance distribution. The convergence analysis and the numerical example are shown in order to evaluate the approximation.

Keywords: Discretization, Distributed parameter system, Frequency response, Ionic-Polymer Metal Composite

1. INTRODUCTION

The new polymer-based soft actuators have been developed recently[1]. The ionic polymer-metal composite (IPMC) is one of such actuators, though its physics is not simple. From experimental observations, it is known that the IPMC actuator is appropriate to be modeled as a distributed parameter system[4]. For example, a distributed RC circuit is an expected candidate for the model of the impedance of the IPMC, because we can observe the rough interface between the polymer and the electrode [3]. For the use of the model in the computer aided analysis and design, the distributed parameter system representation is expected to be approximated by a finite-dimensional system representation.

In this paper, the linear RC distributed circuit is discretized by the mixed finite-element based Hamiltonian discretization method[2]. The discretized model preserves the physical structure of the original distributed system. Using the discretization method, we obtain the lumped RC network model. In order to synthesize the overall impedance (or admittance) from the lumped RC circuits, this paper shows both a state space representation which is suitable for the numerical computation, and a transfer function representation to show that the approximated model converges to the exact model as the order increases. Especially, we consider the case of the constant impedance distribution. Numerical examples show frequency responses of the admittance in order to demonstrate the effectiveness of the discretization.

2. MODEL

2.1 Distributed RC Circuit Model

2.1.1 Governing Equations and the Boundary Condition

Figure 1 shows the distributed RC circuit. The port voltage and the current are v_a and i_a. Let the spatial coordinate be $z \in [0\ L_0]$, where L_0 is the length of the distributed line. The linear impedances are distributed, denoted by Z_1 and Z_2, the series and the parallel impedance density functions, respectively. The governing linear equations in the frequency domain can be derived as[3]:

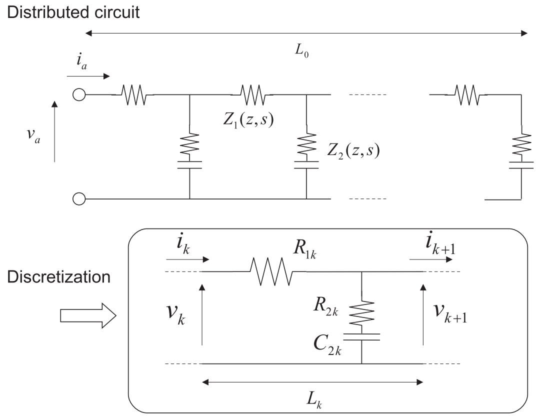

Fig. 1 Discretization of the distributed RC circuit model

$$Z_1(z,s)\tilde{i}(z,s) = -\frac{d\tilde{v}}{dz}(z,s), \tag{1}$$

$$\frac{1}{Z_2(z,s)}\tilde{v}(z,s) = -\frac{d\tilde{i}}{dz}(z,s), \tag{2}$$

where the tilde (˜) represents the function to which Laplace transform is applied. Boundary conditions are given by

$$v|_{z=0} = v_a, \text{ or } i|_{z=0} = i_a \tag{3}$$

$$\tilde{i}|_{z=L_0} = \frac{-1}{Z_1}\left.\frac{d\tilde{v}}{dz}\right|_{z=L_0} = 0. \tag{4}$$

Note that the impedance density functions Z_1 and Z_2 are the spatial function, therefore the general solution of

Eqs. (1) and (2) can not be obtained in general. The exact solution can be obtained only in the case of uniformly distributed impedance density, that is, when Z_1 and Z_2 are constants. We call such a case as constant impedance distribution in this paper.

2.1.2 Exact Solution for the Constant Impedance Distribution

In the case of constant impedance distribution, the general solution of Eqs. (1) and (2) can be easily obtained. Using Eqs. (1), (2), (3) and (4), we get

$$\tilde{i}_a(s) = \frac{\tanh(L_0\sqrt{Z_1/Z_2})}{\sqrt{Z_1 Z_2}}\tilde{v}_a(s)$$

where $\tilde{i}_a(s) := \tilde{i}(0,s)$. The exact solution of the admittance Y_{exact}, defined as a transfer function from $\tilde{v}_a$ to $\tilde{i}_a$, is obtained as:

$$Y_{\text{exact}}(s) = \frac{\tanh(L_0\sqrt{Z_1(s)/Z_2(s)})}{\sqrt{Z_1(s)Z_2(s)}} \tag{5}$$

$$= \sqrt{\frac{C_{20}s}{R_{10}(R_{20}C_{20}s+1)}}\tanh\left(L_0\sqrt{\frac{R_{10}C_{20}s}{R_{20}C_{20}s+1}}\right) \tag{6}$$

where Z_1 and Z_2 can be given by

$$Z_1(s) = R_{10}, \quad Z_2(s) = R_{20} + \frac{1}{C_{20}s}. \tag{7}$$

Note that Y_{exact} is a non-rational function, which comes from the nature of the distributed parameter system.

2.2 Mixed Finite-Element Discretization of the Stokes-Dirac Structure

2.2.1 Hamiltonian Discretization

The distributed RC circuit, which is represented in the previous section, is approximated by the Hamiltonian discretization using a mixed finite-elements method [2]. The discretized model preserves the physical structure, called Stokes-Dirac structure, of the original distributed system.

The distributed line is discretized into N finite-elements. The k-th lumped element is shown in Fig. 1 below. The model consists of the series connection of the lumped RC elements. The element number k is counted from the port to the open end, $k = 1, 2, ..., N$. The parameters of the k-th lumped element are derived as[2]:

$$\frac{1}{\bar{R}_{1k}} = \int_{a_k}^{b_k} * \left(\frac{\omega_2^{a_k b_k}(z)}{R_1(z)}\right)\omega_2^{a_k b_k}(z), \tag{8}$$

$$\bar{R}_{2k} = \int_{a_k}^{b_k} * \left(R_2(z)\omega_1^{a_k b_k}(z)\right)\omega_1^{a_k b_k}(z), \tag{9}$$

$$\frac{1}{\bar{C}_{2k}} = \int_{a_k}^{b_k} * \left(\frac{\omega_1^{a_k b_k}(z)}{C_2(z)}\right)\omega_1^{a_k b_k}(z). \tag{10}$$

where a_k and b_k which satisfy $0 \le a_k < b_k \le L_0$ are the interval of the k-th finite element. $\omega_1^{a_k b_k}(z)$ and $\omega_2^{a_k b_k}(z)$ are the approximation basis for the flow and the effort, respectively. We employed the Hodge star operator $*$, converting any k-form ω on a n-spatial domain $\mathscr{Z}$ to an $(n-k)$-form $*\omega$. In this paper the Riemannian metric is simply the Euclidean inner product corresponding to a choice of local coordinates on $\mathscr{Z}$. Therefore, on the one-dimensional domain $\mathscr{Z}$ with coordinate z, we simply have $*g(z) = g(z)dz$, $*(g(z)dz) = g(z)$ where $g(z)$ is a certain density function.

2.2.2 Approximation by Interpolating One-Forms

The basis one-form $\omega^{a_k b_k}$ is chosen as:

$$\omega^{a_k b_k} = \frac{dz}{L_k} \tag{11}$$

where $L_k = b_k - a_k$. This choice corresponds to the simplest spline approximation [2]. The material approximation [2] is also identical to the spline approximation if the distribution is uniform, that is, $R_1(z)$, $C_2(z)$ and $R_2(z)$ are constants. Substituting Eq. (11) into Eqs. (8), (9) and (10), we obtain:

$$\frac{1}{\bar{R}_{1k}} = \frac{1}{L_k^2}\int_{a_k}^{b_k}\frac{1}{R_1(z)}dz, \tag{12}$$

$$\bar{R}_{2k} = \frac{1}{L_k^2}\int_{a_k}^{b_k} R_2(z)dz, \tag{13}$$

$$\frac{1}{\bar{C}_{2k}} = \frac{1}{L_k^2}\int_{a_k}^{b_k}\frac{1}{C_2(z)}dz. \tag{14}$$

2.2.3 Griding the Finite Elements

For the simplicity, let us employ the equally segmented N's finite elements for the discretization.

$$L_k = \frac{L_0}{N} \quad (k = 1, 2, ..., N) \tag{15}$$

We call this segmentation as equally-spaced segmentation, or uniform grid.

2.3 Linear State Space Representation of the Overall Admittance

In order to connect the each lumped RC circuit, this section discusses the state space representation. The governing equations of the k-th finite element are:

$$i_k - \dot{q}_k - i_{k+1} = 0, \tag{16}$$

$$v_k - \bar{R}_{1k}i_k - v_{k+1} = 0, \tag{17}$$

$$v_{k+1} = \frac{1}{\bar{C}_{2k}}q_k + \bar{R}_{2k}\dot{q}_k. \tag{18}$$

where the state of the system is the charge q_k. Let us derive the transfer function or the state space representation of the k-th system $G_k : [v_k, i_{k+1}]^{\mathrm{T}} \mapsto [i_k, v_{k+1}]^{\mathrm{T}} (k = 1, 2, ..., N)$.

$$G_k(s) = \left[\begin{array}{c|c} A_k & B_k \\ \hline C_k & D_k \end{array}\right], \tag{19}$$

$$A_k = \frac{-1}{(\bar{R}_{1k}+\bar{R}_{2k})\bar{C}_{2k}}, \tag{20}$$

$$B_k = \frac{1}{\bar{R}_{1k}+\bar{R}_{2k}}\begin{bmatrix} 1 & -\bar{R}_{1k} \end{bmatrix}, \tag{21}$$

$$C_k = \frac{-1}{(\bar{R}_{1k}+\bar{R}_{2k})\bar{C}_{2k}}\begin{bmatrix} 1 \\ -\bar{R}_{1k} \end{bmatrix}, \tag{22}$$

$$D_k = \frac{1}{\bar{R}_{1k}+\bar{R}_{2k}}\begin{bmatrix} 1 & \bar{R}_{2k} \\ \bar{R}_{2k} & -\bar{R}_{1k}\bar{R}_{2k} \end{bmatrix}. \tag{23}$$

Overall admittance $\hat{Y}$ can be calculated by the linear fractional transformation (or known as the Redheffer star product) [5] of the each system G_k $(k = 1, 2, ..., N)$. Assuming that the circuit is terminated at the end, i.e., $i_{N+1} \equiv 0$, the admittance $\hat{Y}$ is derived as:

$$\hat{Y} = G_1 \star G_2 \star \cdots \star G_N \star 0 \tag{24}$$

where star ($\star$) denotes the Redheffer star product. The state space representation is suitable for the numerical computation due to the accuracy compared with the transfer function representation.

2.4 Convergence Analysis Using the Transfer Function Representation for the Constant Distribution Case

The state space representation gives us the model suitable for numerical computation, however, it is not trivial whether the approximated finite-dimensional system converges to the original infinite dimensional system or not. In this section, we discuss the convergence of the discretized model in a limited case.

For the constant distribution case, i.e. $R_1(z) = R_{10}$, $R_2(z) = R_{20}$, $C_2(z) = C_{20}$, Eqs. (12), (13) and (14) can be calculated as:

$$\bar{R}_{1k} = L_k R_{10},\ \bar{R}_{2k} = \frac{1}{L_k} R_{20},\ \bar{C}_{2k} = L_k C_{20}. \tag{25}$$

The governing equations of the k-th element can be written in the frequency domain:

$$\tilde{i}_k - \frac{1}{Z_2}\tilde{v}_{k+1} - \tilde{i}_{k+1} = 0, \tag{26}$$

$$\tilde{v}_k - Z_1 \tilde{i}_k - \tilde{v}_{k+1} = 0, \tag{27}$$

where $Z_1 = R_{10}L_0/N$, $Z_2 = R_{20}N/L_0 + \frac{1}{sC_{20}L_0/N}$.

Define Y_k as:

$$\tilde{i}_k = Y_k \tilde{v}_k. \tag{28}$$

Substituting Eq. (28) into Eqs. (26) and (27), and eliminating $\tilde{i}$ and $\tilde{v}$, we obtain:

$$Y_k = \frac{1 + Y_{k+1}Z_2}{Z_1 + Z_2 + Y_{k+1}Z_1Z_2}. \tag{29}$$

Eq. (29) is a sequence or a nonlinear difference equation with respect to Y_k $(k = N+1, N, N-1, ..., 1)$. The initial condition of the sequence Eq. (29) is given by:

$$Y_{N+1} = 0, \tag{30}$$

due to the boundary condition $i_{N+1} \equiv 0$ as shown in the previous section. The sequence of Eq. (29) with the initial condition Eq. (30) can be solved as:

$$Y_k = \frac{2N(1 - S_{1k}S_{2k})}{(P_1(P_1 + 4N^2P_2))^{\frac{1}{2}}(1 + S_{1k}S_{2k})} \tag{31}$$

$$S_{1k} := \left(\frac{P_1(P_1 + 2N^2P_2 - (P_1(P_1 + 4N^2P_2))^{\frac{1}{2}})}{N^3P_2}\right)^{N-k} \tag{32}$$

$$S_{2k} := \left(\frac{P_1(P_1 + 2N^2P_2 + (P_1(P_1 + 4N^2P_2))^{\frac{1}{2}})}{N^3P_2}\right)^{k-N} \tag{33}$$

Table 1 Parameters used in the numerical examples

L_0	R_{10}	R_{20}	C_{20}
0.05[m]	10^3[Ω/m]	10^{-3}[Ωm]	10[F/m]

where $P_1 := Z_1N$, $P_2 := Z_2/N$. Substituting $k = 1$ into Eq. (31), the overall admittance $\hat{Y}$ is obtained as:

$$\hat{Y} = Y_1. \tag{34}$$

We can confirm that the approximated admittance $Y_1 (= \hat{Y})$ converges to the exact solution Y_{exact} of Eq. (6) as $N \to \infty$.

Proposition 1: Y_1 of Eq. (31) converges to Y_{exact} of Eq. (6) as $N \to \infty$:

$$\lim_{N\to\infty} Y_1 = \frac{\tanh\left((P_1/P_2)^{\frac{1}{2}}\right)}{(P_1P_2)^{\frac{1}{2}}} = Y_{\text{exact}}. \tag{35}$$

See Appendix A for the proof of Eq. (35).

3. NUMERICAL EXAMPLE

The discretized model is evaluated by observing the differences of the frequency response between the discretized model and the exact solution. The star product is calculated by `lft` function of MATLAB in order to synthesize the overall admittance $\hat{Y}$. Table 1 shows the parameters used in the numerical examples.

Figure 2 shows the bode diagram of the impedance. The solid line is the exact solution, the dashed or the chained lines are the discretized models. The dashed line is the case of $N = 50$, the chained line is for $N = 10$. The responses of the discretized models well fit the exact solution at the low frequency, though a little differ from the exact solution at the high frequency. The error decreases as the approximation order N increases. The characteristic property of a transmission line, that the phase is about $\pi/4$[rad] (-45[deg]) and that the gain slope is $1/2$, can be observed around at 1[rad/s]. The bode diagram of the error is also shown in Fig. 3. The gain shape of the error is similar to the impedance shown in Fig. 2. The error is smaller when the frequency is lower. This is because the total capacitance is preserved in the approximated model, therefore the discretized model is identical to the distributed model at the zero frequency.

4. CONCLUSION

This paper discussed the discretization of the distributed RC circuit model which is the candidate of the impedance model of ionic polymer actuators. The Hamiltonian discretization based on mixed-finite element method was shown. The state space representation and the transfer function representation were derived for the computation and the analysis, respectively. In the numerical example, the response of the approximated model well fit the exact solution at the low frequency. We also showed the response of the limit of the approximated

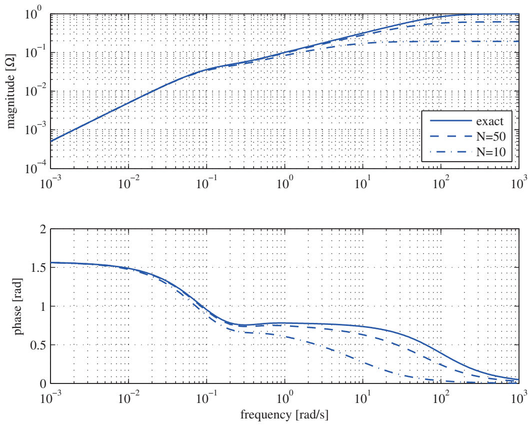

Fig. 2 Bode diagram of the admittance for the constant impedance distribution case

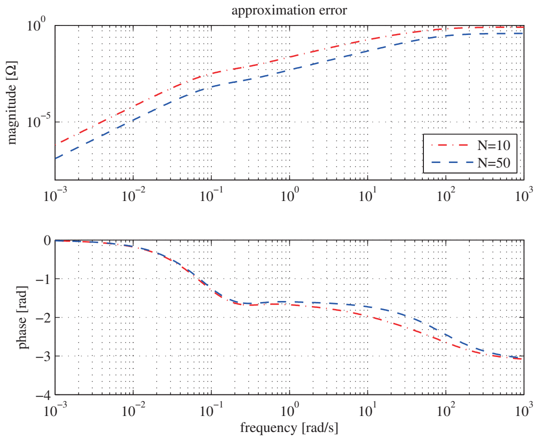

Fig. 3 Bode diagram of the approximation error

model converged to the exact solution as the segmentation increased.

Acknowledgment This work was supported by Japan Ministry of Education, Science, Sports and Culture, Grant-in-Aid for Young Scientists (B) 19760169.

REFERENCES

[1] Y. Bar-Cohen, ed., *Electroactive Polymer (EAP) Actuators as Artificial Muscles: Reality, Potential, and Challenges*, SPIE Press, 2nd ed., (2004).

[2] G. Golo, V. Talasila, A. van der Schaft, B. Maschke, "Hamiltonian Discretization of Boundary Control Systems," Automatica, **40**, pp. 757–771, (2004)

[3] K.Takagi, Y.Nakabo, Z.W.Luo, K.Asaka, "On a distributed parameter model for electrical impedance of ionic polymer," Proc. of SPIE, **6524**, 652416-1/652416-8 (2007)

[4] G.Nishida, K.Takagi, B.Maschke, Z.W.Luo, "Multi-Scale Distributed Port-Hamiltonian Representation of Ionic Polymer-Metal Composite (IPMC)", Proc. the 17th World Congress the IFAC, pp.2300–2305 (2008)

[5] K.Zhou, J.Doyle, Essentials of Robust Control, pp.178–180, Prentice Hall, (1998)

APPENDIX

A PROOF OF THE PROPOSITION 1

Considering the fact:

$$e = \lim_{n\to\infty}\left(1+\frac{1}{n}\right)^n, \quad n \in \mathbb{N},$$

we have the following lemma.

Lemma 1:

$$\lim_{n\to\infty}\left(1+\frac{\kappa}{n}+O\left(\frac{1}{n^2}\right)\right)^n = e^{\kappa}, \quad \kappa \in \mathbb{C}$$

Proof of Proposition 1: Substituting $k = 1$ into Eq. (31) to obtain Y_1, we have:

$$Y_1 = \frac{1}{(P_1(\frac{P_1}{4N^2}+P_2))^{\frac{1}{2}}}\frac{1-S_{10}S_{20}}{1+S_{10}S_{20}}. \tag{36}$$

Taking the limit of the first term of the right hand side of Eq. (36), we obtain:

$$\lim_{N\to\infty}\frac{1}{(P_1(\frac{P_1}{4N^2}+P_2))^{\frac{1}{2}}} = \frac{1}{(P_1P_2)^{\frac{1}{2}}}. \tag{37}$$

Canceling the common factors of S_{10} and S_{20}, the second term of Eq. (36) can be approximated as:

$$\frac{1-S_{10}S_{20}}{1+S_{10}S_{20}} = \frac{1-Q_1Q_2}{1+Q_1Q_2} \tag{38}$$

where

$$Q_1 := \left(1-\left(\frac{P_1}{P_2}\right)^{\frac{1}{2}}\frac{1}{N}+O(\frac{1}{N^2})\right)^N,$$

$$Q_2 := \left(1+\left(\frac{P_1}{P_2}\right)^{\frac{1}{2}}\frac{1}{N}+O(\frac{1}{N^2})\right)^{-N}.$$

Using Lemma 1, we obtain:

$$\lim_{N\to\infty} Q_1 = e^{-\left(\frac{P_1}{P_2}\right)^{\frac{1}{2}}},$$

$$\lim_{N\to\infty} Q_2 = e^{\left(\frac{P_1}{P_2}\right)^{\frac{1}{2}}}.$$

The limit of the right hand side of Eq. (38) becomes:

$$\lim_{N\to\infty}\frac{1-S_{10}S_{20}}{1+S_{10}S_{20}} = \frac{1-e^{-\left(\frac{P_1}{P_2}\right)}}{1+e^{-\left(\frac{P_1}{P_2}\right)}} = \tanh\left(\left(\frac{P_1}{P_2}\right)^{\frac{1}{2}}\right). \tag{39}$$

Using Eqs. (36), (37) and (39), we have Eq. (35). □